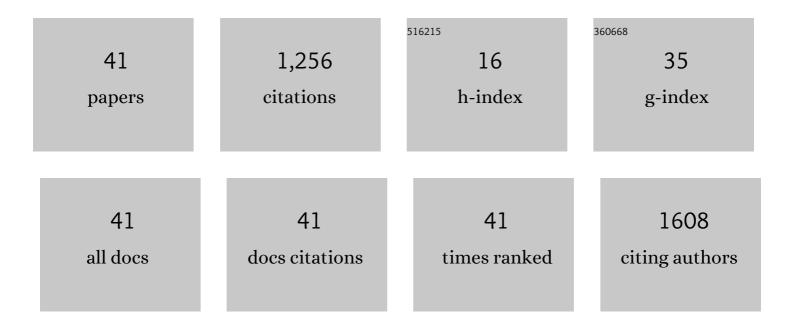
Nathan R Miller

List of Publications by Year in descending order

Source: https://exaly.com/author-pdf/3198524/publications.pdf Version: 2024-02-01



#	Article	IF	CITATIONS
1	Iodide in CTAB Prevents Gold Nanorod Formation. Langmuir, 2009, 25, 9518-9524.	1.6	198
2	Mass-production of Cambro–Ordovician quartz-rich sandstone as a consequence of chemical weathering of Pan-African terranes: Environmental implications. Earth and Planetary Science Letters, 2005, 240, 818-826.	1.8	193
3	Mg and Ca isotope signatures of authigenic dolomite in siliceous deep-sea sediments. Earth and Planetary Science Letters, 2015, 419, 32-42.	1.8	111
4	Detrital zircon U–Pb geochronology of Cryogenian diamictites and Lower Paleozoic sandstone in Ethiopia (Tigrai): Age constraints on Neoproterozoic glaciation and crustal evolution of the southern Arabian–Nubian Shield. Precambrian Research, 2007, 154, 88-106.	1.2	85
5	â^¼750 Ma banded iron formation from the Arabian-Nubian Shield—Implications for understanding neoproterozoic tectonics, volcanism, and climate change. Precambrian Research, 2013, 239, 79-94.	1.2	74
6	Evidence for ca. 560Ma Ediacaran glaciation in the Kahar Formation, central Alborz Mountains, northern Iran. Gondwana Research, 2016, 31, 164-183.	3.0	69
7	A Late Neoproterozoic (â^1⁄4630 Ma) high-magnesium andesite suite from southern Israel: implications for the consolidation of Gondwanaland. Earth and Planetary Science Letters, 2004, 218, 475-490.	1.8	66
8	Significance of the Tambien Group (Tigrai, N. Ethiopia) for Snowball Earth events in the Arabian–Nubian Shield. Precambrian Research, 2003, 121, 263-283.	1.2	52
9	Origin of garnet in aplite and pegmatite from Khajeh Morad in northeastern Iran: A major, trace element, and oxygen isotope approach. Lithos, 2014, 208-209, 378-392.	0.6	31
10	Cryogenian slate-carbonate sequences of the Tambien Group, Northern Ethiopia (I): Pre-"Sturtian― chemostratigraphy and regional correlations. Precambrian Research, 2009, 170, 129-156.	1.2	29
11	Compositional gradients surrounding spherulites in obsidian and their relationship to spherulite growth and lava cooling. Bulletin of Volcanology, 2012, 74, 1865-1879.	1.1	29
12	Case studies on the utility of sequential carbonate leaching for radiogenic strontium isotope analysis. Chemical Geology, 2018, 497, 88-99.	1.4	28
13	Fin spine chemistry as a non-lethal alternative to otoliths for stock discrimination in an endangered catfish. Marine Ecology - Progress Series, 2019, 614, 147-157.	0.9	27
14	Did the transition to plate tectonics cause Neoproterozoic Snowball Earth?. Terra Nova, 2018, 30, 87-94.	0.9	25
15	High resolution profiles of elements in Atlantic tarpon (Megalops atlanticus) scales obtained via cross-sectioning and laser ablation ICP-MS: a literature survey and novel approach for scale analyses. Environmental Biology of Fishes, 2015, 98, 2223-2238.	0.4	23
16	Elements of time and place: manganese and barium in shark vertebrae reflect age and upwelling histories. Proceedings of the Royal Society B: Biological Sciences, 2018, 285, 20181760.	1.2	22
17	Spherulites as in-situ recorders of thermal history in lava flows. Geology, 2015, 43, 647-650.	2.0	18
18	Population structure and habitat connectivity of Genidens genidens (Siluriformes) in tropical and subtropical coasts from Southwestern Atlantic. Estuarine, Coastal and Shelf Science, 2020, 242, 106839.	0.9	17

NATHAN R MILLER

#	Article	IF	CITATIONS
19	The interplay between ceria particle size, reducibility, and ethanol oxidation activity of ceria-supported gold catalysts. Reaction Chemistry and Engineering, 2018, 3, 75-85.	1.9	15
20	Silversides (Odontesthes bonariensis) reside within freshwater and estuarine habitats, not marine environments. Estuarine, Coastal and Shelf Science, 2018, 205, 123-130.	0.9	15
21	The potential of near-entrance stalagmites as high-resolution terrestrial paleoclimate proxies: Application of isotope and trace-element geochemistry to seasonally-resolved chronology. Geochimica Et Cosmochimica Acta, 2018, 235, 55-75.	1.6	13
22	Natal origin of Pacific bluefin tuna from the California Current Large Marine Ecosystem. Biology Letters, 2020, 16, 20190878.	1.0	11
23	Spatiotemporal Stability of Trace and Minor Elemental Signatures in Early Larval Shell of the Northern Quahog (Hard Clam) <i>Mercenaria mercenaria</i> . Journal of Shellfish Research, 2014, 33, 247-255.	0.3	10
24	Chapter 21 The Tambien Group, Northern Ethiopia (Tigre). Geological Society Memoir, 2011, 36, 263-276.	0.9	9
25	Microchemistry of juvenile Mercenaria mercenaria shell: implications for modeling larval dispersal. Marine Ecology - Progress Series, 2012, 465, 155-168.	0.9	9
26	Strontium isotope constraints on solute sources and mixing dynamics in a large impoundment, South-Central USA. Chemical Geology, 2011, 285, 203-214.	1.4	8
27	Effects of sample cleaning and storage on the elemental composition of shark vertebrae. Rapid Communications in Mass Spectrometry, 2017, 31, 2073-2080.	0.7	8
28	Fin spine metals by LA-ICP-MS as a method for fish stock discrimination of Genidens barbus in anthropized estuaries. Fisheries Research, 2020, 230, 105625.	0.9	8
29	Neoproterozoic Glaciation—Snowball Earth Hypothesis. , 2021, , 546-556.		7
30	Improved accuracy of U-series and radiocarbon dating of ostrich eggshell using a sample preparation method based on microstructure and geochemistry: A study from the Middle Stone Age of Northwestern Ethiopia. Quaternary Science Reviews, 2020, 247, 106525.	1.4	7
31	Speculations Linking Monazite Compositions to Origin: Llallagua Tin Ore Deposit (Bolivia). Resources, 2017, 6, 36.	1.6	6
32	Heterogeneity in Mixed Cerium Oxides and Its Influence on the Behavior of Gold Catalysts for the Selective Oxidation of Ethanol. Journal of Physical Chemistry C, 2017, 121, 19269-19279.	1.5	5
33	Cooling rates of mid-ocean ridge lava deduced from clinopyroxene spherulites. Journal of Volcanology and Geothermal Research, 2014, 282, 1-8.	0.8	4
34	lon microprobe ²³² Th- ²⁰⁸ Pb ages from high common Pb monazite, Morefield Mine, Amelia County, Virginia: Implications for Alleghanian tectonics. Numerische Mathematik, 2016, 316, 470-503.	0.7	4
35	Neoproterozoic Rosetta Gabbro from northernmost Arabian–Nubian Shield, south Jordan: Geochemistry and petrogenesis. Lithos, 2017, 284-285, 545-559.	0.6	4
36	Fluids along the North Anatolian Fault, Niksar basin, north central Turkey: Insight from stable isotopic and geochemical analysis of calcite veins. Journal of Structural Geology, 2017, 101, 58-79.	1.0	4

NATHAN R MILLER

#	Article	IF	CITATIONS
37	Ontogenetic Patterns of Elemental Tracers in the Vertebrae Cartilage of Coastal and Oceanic Sharks. Frontiers in Marine Science, 2021, 8, .	1.2	4
38	Integrated use of otolith shape and microchemistry to assess Genidens barbus fish stock structure. Estuarine, Coastal and Shelf Science, 2021, 261, 107560.	0.9	3
39	Origin and Evolution of Oscillatory Zoned Garnet From Kasva Skarn, Northeast Tafresh, Iran. Canadian Mineralogist, 2018, 56, 15-37.	0.3	2
40	Hydroclimate response in Texas and Gulf of Mexico to rapid warming during the last deglacial: High-resolution speleothem proxy and monitoring evidence. Quaternary Science Reviews, 2021, 273, 107244.	1.4	2
41	Evolution of the Arabian Nubian Shield and Snowball Earth. Regional Geology Reviews, 2021, , 153-194.	1.2	1